

# An SSD-based eigensolver for spectral analysis on billion-node graphs

Da Zheng, Randal Burns  
*Department of Computer Science*  
*Johns Hopkins University*

Joshua Vogelstein  
*Institute for Computational Medicine*  
*Department of Biomedical Engineering*  
*Johns Hopkins University*

Carey E. Priebe  
*Department of Applied Mathematics and Statistics*  
*Johns Hopkins University*

Alexander S. Szalay  
*Department of Physics and Astronomy*  
*Johns Hopkins University*

## Abstract

Many eigensolvers such as ARPACK and Anasazi have been developed to compute eigenvalues of a large sparse matrix. These eigensolvers are limited by the capacity of RAM. They run in memory of a single machine for smaller eigenvalue problems and require the distributed memory for larger problems.

In contrast, we develop an SSD-based eigensolver framework called FlashEigen, which extends Anasazi eigensolvers to SSDs, to compute eigenvalues of a graph with hundreds of millions or even billions of vertices in a single machine. FlashEigen performs sparse matrix multiplication in a semi-external memory fashion, i.e., we keep the sparse matrix on SSDs and the dense matrix in memory. We store the entire vector subspace on SSDs and reduce I/O to improve performance through caching the most recent dense matrix. Our result shows that FlashEigen is able to achieve 40%-60% performance of its in-memory implementation and has performance comparable to the Anasazi eigensolvers on a machine with 48 CPU cores. Furthermore, it is capable of scaling to a graph with 3.4 billion vertices and 129 billion edges. It takes about four hours to compute eight eigenvalues of the billion-node graph using 120 GB memory.

## 1 Introduction

Spectral analysis [] is a fundamental tool for both graph analysis and other areas of data mining. Essentially, it computes eigenvalues and eigenvectors of graphs to infer properties of graphs. spectral clustering [17, 22], triangle counting [24]. Many real-world graphs are massive: Facebook’s social network has billions of vertices and today’s web graph is even much larger.

It is computationally expensive to compute all eigenvalues and eigenvectors of a large matrix. The computation complexity is  $O(n^3)$  on a square matrix [19], where  $n$  is the number of rows and columns of the matrix. When

the size of a matrix grows to millions or even billions of rows and columns, it becomes prohibitive to compute all eigenvalues and eigenvectors.

Numerous algorithms [14, 7, 21, 4] have been developed to compute a small number of eigenpairs. The current popular eigensolver packages such as ARPACK [15] and Anasazi [5] have state-of-art eigensolvers capable of computing a few eigenvalues with certain properties such as the eigenvalues of the largest or smallest magnitude. All of these eigensolvers perform a sequence of sparse matrix multiplication to construct and update a vector subspace  $S \in \mathbb{R}^{n \times m}$ , where  $n$  is the size of the eigenproblem and  $m$  is the subspace size [4]. In addition, they perform matrix operations on the vector subspace. When computing eigenpairs of a graph at the billion scale, neither the sparse matrix that represents a graph nor the vector subspace fits in the RAM of a single machine.

It is challenging to implement an efficient kernel of sparse matrix multiplication for many real-world graphs. Sparse matrix multiplication on these graphs induces many small random memory access due to near-random vertex connection. It may suffer from load imbalancing because of the power-law distribution in vertex degree. Furthermore, graphs cannot be clustered or partitioned effectively [16] to localize access.

Large-scale eigendecomposition is generally solved in a large cluster [5, 9], where the aggregate memory is sufficient to store the sparse matrix and the vector subspace. Sparse matrix multiplication on graphs in distributed memory leads to significant network communication and is usually bottlenecked by the network. As such, this operation requires fast network to achieve performance. However, a supercomputer or a large cluster with fast network communication is not accessible to many people.

We build FlashEigen, an external-memory eigensolver, on top of a user-space filesystem called SAFS [29] to solve a large eigenproblem with SSDs in a single machine. Instead of developing a new eigensolver

from scratch, we leverage the Anasazi framework and implement SSD-based matrix operations for the framework. FlashEigen is specifically optimized for the Block Krylov-Schur [21] eigensolver because it is the fastest and generates the least I/O among the Anasazi eigensolvers when computing eigenvalues of many power-law graphs. The Anasazi eigensolvers implement a block extension, which enables the eigensolvers to update multiple vectors in the subspace in each iteration to increase computation density and amortize I/O overhead. As a result, the eigensolvers require sparse matrix dense matrix multiplication (SpMM). Given a graph with hundreds of millions of vertices or even billions of vertices, the vector subspace constructed by the eigensolvers requires very large storage size, usually much larger than the sparse matrix. Therefore, FlashEigen stores the entire vector subspace on SSDs.

Although SSDs can deliver high IOPS and sequential I/O throughput, we have to overcome many technical challenges to construct an external-memory eigensolver with performance comparable to in-memory eigensolvers. First, it is challenging to achieve the maximal I/O throughput, on the order of ten gigabytes, from a large array of commodity SSDs, due to many overheads from the operating system. Even achieving the maximal I/O throughput, SSDs are still an order of magnitude slower than DRAM in throughput. Furthermore, SSDs wear out after we write data to them. For example, some enterprise SSDs [18] only allows one DWPD (diskful writes per day). Writing too much data to these SSDs drastically shortens their lives and increases operation cost.

We perform SpMM in a semi-external memory (SEM) fashion, which keeps the sparse matrix on SSDs and dense matrices in memory. This operation streams rows in the sparse matrix to memory and multiplies with the dense matrix in memory, which generates sequential I/O and allows us to yield maximal I/O throughput from SSDs. While maximizing the I/O throughput, we also compress the sparse matrix to further accelerate retrieving the sparse matrix from SSDs. The SEM strategy incorporates well with in-memory optimizations for SpMM. We deploy multiple in-memory optimizations specifically designed for power-law graphs. For example, we assign partitions of the sparse matrix dynamically to threads for load balancing, deploy cache blocking to increase CPU cache hits, partition and evenly distribute the dense matrix to NUMA nodes to fully utilize the memory bandwidth of a NUMA machine.

We deploy optimizations on dense matrix operations to reduce I/O and fully utilize the I/O bandwidth of the SSDs. Thanks to the block extension of the Anasazi eigensolvers, we group multiple vectors together into a column-major dense matrix and store each dense matrix

in a separate SAFS file for efficient I/O access to any vectors in the subspace. When accessing a large number of dense matrices in a single operation, we group dense matrices to constrain memory consumption of the matrix operation to improve its scalability. To reduce I/O and alleviate SSD wear out, we use deploy lazy evaluation and cache the most recent dense matrix in the subspace.

Our result shows that for many real-world sparse graphs, the SSD-based eigensolver is able to achieve 40%-60% performance of its in-memory implementation and has performance comparable to the Anasazi eigensolver on a machine with 48 CPU cores for computing various numbers of eigenvalues. We further demonstrate that the SSD-based eigensolver is capable of scaling to a graph with 3.4 billion vertices and 129 billion edges. It takes about 4 hours to compute eight eigenvalues of the billion-node graph and use 120 GB memory. We conclude that our solution offers new design possibilities for large-scale eigendecomposition, replacing memory with larger and cheaper SSDs and processing bigger problems on fewer machines.

## 2 Related Work

Anasazi [5] is an eigensolver framework in the Trilinos project [10]. This framework implements block extension of multiple eigensolver algorithms such as Block Krylov-Schur method [21], Block Davidson method [4] and LOBPCG [4]. This is a very flexible framework that allows users to redefine sparse matrix dense matrix multiplication and dense matrix operations. By default, Anasazi uses the matrix implementations in Trilinos that run in the distributed memory.

Arpack [15] is another state-of-art eigensolver commonly used by multiple numeric computation frameworks such as Matlab. This eigensolver implements the implicitly restarted arnoldi method [20]. Arpack only allows users to redefine sparse matrix vector multiplication. Its dense matrix operations by default run in serial.

Sparse matrix vector multiplication (SpMV) and sparse matrix dense matrix multiplication (SpMM) are an important operation in numeric computation and are well studied in the literature. For example, Williams et. al [26] described multiple optimizations for sparse matrix vector multiplication in multicore architecture. Yoo et. al [28] and Boman et. al [6] optimized SpMV for large scale-free graphs using 2D graph partitioning. Aktulga et. al [2] optimized sparse matrix dense matrix multiplication with cache blocking. In contrast, we further advance sparse matrix dense matrix multiplication with a focus on optimizations for external memory.

FlashGraph [30] is a general graph analysis framework. It performs graph algorithms in a semi-external memory fashion [1], i.e., it keeps vertex state in memory

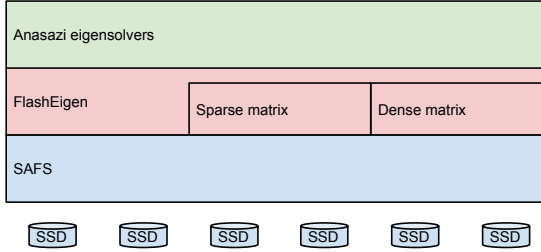


Figure 1: The architecture of FlashEigen.

and edge lists on SSDs. It is specifically optimized for graph algorithms that has a fraction of vertices running in each iteration. This design prevents FlashGraph from performing some optimizations for sparse matrix multiplication as shown in this paper.

HEIGEN [12] is an eigensolver implemented with MapReduce [8] to compute eigenpairs for spectral graph analysis. HEIGEN implements a basic Lanczos algorithm [14] with selective orthogonalization from scratch. In contrast, our approach extends the state-of-art implementations to SSDs. By integrating many SSDs to a single machine, our approach can compete with a cluster.

Zhou et al. [31] implemented an LOBPCG [4] eigensolver in an SSD cluster. Their implementation targets nuclear many-body Hamiltonian matrices, which are much denser and have smaller dimensions than many sparse graphs. Therefore, their solution stores the sparse matrix on SSDs and keep the entire vector subspace in RAM. Their solution also focus on optimizations in the distributed environment. In contrast, we store both the sparse matrix and the vector subspace on SSDs due to the large number of vertices in our target graphs. We focus on external-memory optimizations in a single machine.

### 3 Design

FlashEigen is an external-memory eigensolver framework optimized for any fast I/O devices such as a large SSD array to compute eigenvalues of sparse graphs (Figure 1). We build FlashEigen on top of SAFS, a user-space filesystem, to fully utilize the I/O throughput of a large SSD array. Instead of implementing eigenvalue algorithms from scratch, we integrate FlashEigen with the Anasazi framework to compute eigenvalues. The Anasazi framework implements multiple state-of-art eigenvalue algorithms and provides users a flexible programming interface to redefine both sparse and dense matrix operations required by the eigenvalue algorithms. FlashEigen stores both sparse and dense matrices in SAFS and focuses on optimizing the matrix operations required by the Anasazi eigensolvers for SSDs.

### 3.1 Eigensolver algorithm

**Algorithm 1** Pseudo code of a generic eigenvalue algorithm that compute eigenvalues of a square matrix  $A$  with  $n$  rows and columns.

- 
- 1: **for**  $i = 0, 1, \dots$ , until convergence **do**
  - 2:     (1) Update the subspace  $S \in \mathbb{R}^{n \times m}$ ,
  - 3:     (2) Solve the projected eigenproblem  $S^T A S y = S^T S y \theta$ .
  - 4:     (3) Compute the residual:  $r = Kx - x\theta$ , where
  - 5:          $x = S y$  (Ritz vector),  $\theta = \rho(x)$  (Ritz value).
  - 6:     (4) Test the convergence of a Ritz pair  $(x, \rho(x))$ .
  - 7: **end for**
- 

The state-of-art eigenvalue algorithms compute eigenvalues with iterative methods. Algorithm 1 shows the general steps used by the eigenvalue algorithms. Step (1) constructs a vector subspace  $S \in \mathbb{R}^{n \times m}$ , where  $n$  is the number of rows and columns of a sparse matrix and  $m$  is the number of vectors in the subspace. When computing eigenvalues of a sparse graph, two key operations in this step are sparse matrix multiplication to construct the subspace and reorthogonalization to correct floating-point rounding errors. Step (2) projects the large sparse matrix to a much smaller matrix with only  $m$  rows and  $m$  columns, which can be solved by other eigensolvers such as the one in LAPACK [3]. Step (3) projects the solution of the small eigenvalue problem back to the original eigenvalue problem. Step (4) tests whether the projected solution fulfills the precision requirement given by users. If not, the algorithm adjusts the vector subspace, returns to step (1) and continues the process.

The block extension implemented in the Anasazi eigensolvers updates multiple vectors in the subspace in an iteration. This optimization leads to sparse matrix dense matrix multiplication, which increases computation density to improve performance, as well as a set of dense matrix operations instead of vector operations. The number of vectors to be updated together is determined by the *block size*, denoted by  $b$ . The subspace size  $m$  is  $b \times NB$ , where  $NB$  is the number of blocks.

### 3.2 SAFS

SAFS [29] is a user-space filesystem for a high-speed SSD array in a NUMA (non-uniform memory architecture) machine. It is implemented as a library and runs in the address space of its application. It is deployed on top of the Linux native filesystem. SAFS was originally designed for optimizing small I/O accesses. However, sparse matrix multiplication and dense matrix operations generate much fewer but much larger I/O. Therefore, we provide additional optimizations to maximize sequential I/O throughput from a large SSD array.

The latency of a thread context switch becomes noticeable on a high-speed SSD array under a sequential I/O workload and it becomes critical to avoid thread context switch to gain I/O performance. If the computation in application threads does not saturate CPU, SAFS will put the application threads into sleep while they are waiting for I/O. This results in many thread context switches and underutilization of both CPU and SSDs. To saturate I/O, an application thread issues asynchronous I/O and poll for I/O to avoid thread context switches after completing all computation available to it.

To better support access to many relatively small files simultaneously, SAFS stripes data in a file across SSDs with a different striping order for each file. This strategy stores data from multiple files evenly across SSDs and improves I/O utilization. Due to the sequential I/O workload, FlashEigen stripes data across SSDs with a large block size, on the order of megabytes, to increase I/O throughput and potentially reduce write amplification on SSDs [23]. Such a large block size may cause storage skew for small files on a large SSD array if every file stripes data in the same order. Using the same striping order for all files may also cause skew in I/O access. Therefore, SAFS generates a random striping order for each file to evenly distribute I/O among SSDs when a file is created. SAFS stores the striping order with the file for future data retrieval.

### 3.3 Sparse matrix multiplication

Sparse matrix multiplication is one of the most computationally expensive operations in an eigensolver. Applying this operation on real-world graphs usually leads to many random memory accesses and its performance is usually limited by the random memory performance of DRAM. The block extension in the Anasazi eigensolvers enables sparse matrix dense matrix multiplication to increase data locality and computation density and improve overall performance of an eigensolver.

To scale sparse matrix multiplication to a sparse graph with billions of vertices, we perform this operation in semi-external memory (SEM). That is, we keep dense matrices in memory and the sparse matrix on SSDs. This strategy enables nearly in-memory performance while achieving the scalability in proportion to the ratio of edges to vertices in a graph.

#### 3.3.1 The sparse matrix format

The state-of-art numeric libraries store a sparse matrix in compressed row storage (CSR) or compressed column storage (CSC) format. However, these formats incur many CPU cache misses in sparse matrix multiplication on many real-world graphs due to their nearly random

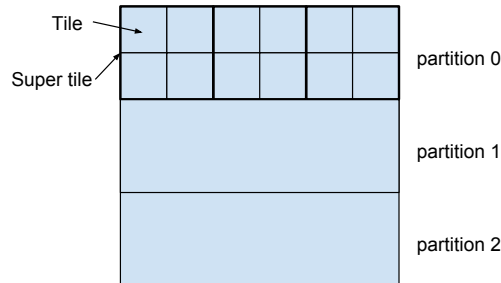


Figure 2: The format of a sparse matrix in FlashEigen.

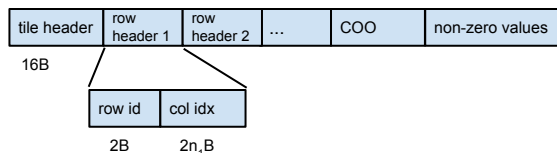


Figure 3: The storage format of a tile in a sparse matrix.

vertex connection. They also require a relatively large storage size. For a graph with billions of edges, we have to use eight bytes to store the row and column indices. For semi-external memory sparse matrix multiplication, SSDs may become the bottleneck if a sparse matrix has a large storage size. Therefore, we need to use an alternative format for sparse matrices to increase CPU cache hits and reduce the amount of data read from SSDs.

To increase CPU cache hits, we deploy cache blocking [11] and store non-zero entries of a sparse matrix in tiles (Figure 2). When a tile is small, the rows from the input and output dense matrices involved in the multiplication with the tile are always kept in the CPU cache during the multiplication. The optimal tile size should fill the CPU cache with the rows of the dense matrices involved in the multiplication with the tile and is affected by the number of columns of the dense matrices, which is chosen by users. Instead of generating a sparse matrix with different tile sizes optimized for different numbers of columns in the dense matrices, we use a relatively small tile size and rely on the runtime system to optimize for different numbers of columns (in section 3.3.3). In the semi-external memory, we expect that the dense matrices do not have more than eight columns in sparse matrix multiplication. Therefore, we use the tile size of  $16K \times 16K$  by default to balance the matrix storage size and the adaptability to different numbers of columns.

To reduce the overall storage size of a sparse matrix, we use a compact format to store non-zero entries in a tile. In very sparse matrices such as many real-world graphs, many rows in a tile do not have any non-zero entries. The CSR (CSC) format requires an entry for each row (column) in the row (column) index. Therefore, the CSR or CSC format wastes space when storing elements in a tile. Instead, we only keep data for rows with non-

zero entries in a tile shown in Figure 3 and refer to this format as SCSR (Super Compressed Row Storage). This format maintains a row header for each non-empty row. A row header has an identifier to indicate the row number, followed by column indices. The most significant bit of the identifier is always set to 1, while the most significant bit of a column index entry is always set to 0. As such, we can easily distinguish a row identifier from a column index entry and determine the end of a row. Thanks to the small size of a tile, we use two bytes to further store a row number and a column index entry to reduce the storage size. Since the most significant bit is used to indicate the beginning of a row, this format allows a maximum tile size of  $32K \times 32K$ .

For many real-world graphs, many rows in a tile have only one non-zero entry, thanks to the sparsity of the graphs and nearly random vertex connection. Iterating over single-entry rows requires to test the end of a row for every non-zero entry, resulting in many extra conditional jump CPU instructions in sparse matrix multiplication. In contrast, the coordinate format (COO) is more suitable for storing these single-entry rows. It does not increase the storage size but significantly reduces the number of conditional jump instructions when we iterate them. As a result, we hybrid SCSR and COO to store non-zero entries in a tile with COO stored behind the row headers of SCSR. All non-zero entries are stored together at the end of a tile.

We organize tiles in a sparse matrix in tile rows and maintain a matrix index for them. Each entry of the index stores the location of a tile row on SSDs to facilitate random access to tile rows. This is useful for parallelizing sparse matrix multiplication. Because a tile contains thousands of rows, the matrix index requires a very small storage size even for a billion-node graph. We keep the entire index in memory during sparse matrix multiplication.

### 3.3.2 The dense matrix format for SpMM

Dense matrices in sparse matrix multiplication are tall-and-skinny (TAS) matrices with millions or even billions of rows but only several columns. The number of rows in a dense matrix is determined by the number of vertices in a sparse graph and the number of columns is determined by the *block size* in an eigensolver with the block extension. The dense matrix is kept in memory for semi-external memory (SEM) sparse matrix dense matrix multiplication (SpMM), so the size of the dense matrix governs the memory consumption of SpMM. Given the limited amount of RAM in a machine, the number of columns in a dense matrix has to be small.

For a non-uniform memory architecture (NUMA), we partition the input dense matrix horizontally and store

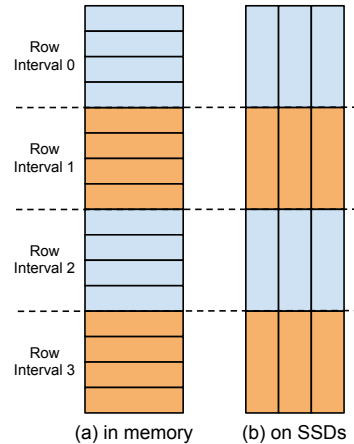


Figure 4: The data layout of tall-and-skinny (TAS) dense matrices. A TAS dense matrix is partitioned horizontally into many row intervals. (a) For an in-memory matrix, row intervals are stored across NUMA nodes and elements are stored in row-major order; (b) for an SSD-based matrix, elements inside a row interval are stored in column-major order.

partitions evenly across NUMA nodes to fully utilize the bandwidth of memory and inter-processor links in sparse matrix multiplication. The NUMA architecture is prevalent in today’s multi-processor servers, where each processor connects to its own memory banks. As shown in Figure 4 (a), we assign multiple contiguous rows in a row interval to a partition, which is assigned to a NUMA node. A row interval always has  $2^i$  rows for efficiently locating a row with bit operations. The row interval size is also multiple of the tile size of a sparse matrix so that multiplication on a tile only needs to access rows from a single row interval. We store elements in a row interval in row-major order to increase data locality in SpMM.

### 3.3.3 Execution of sparse matrix multiplication

We perform sparse matrix dense matrix multiplication in semi-external memory and optimize it for different numbers of columns in the dense matrices. Thanks to the semi-external memory execution, sparse matrix multiplication streams data in the sparse matrix from SSDs, which maximizes I/O throughput of the SSDs.

We partition a sparse matrix horizontally for parallelization and assign multiple contiguous tile rows to the same partition (Figure 2). The number of tile rows assigned to a partition is determined at runtime based on the number of columns in the input dense matrix. A thread reads a partition of the sparse matrix asynchronously from SSDs. Once a partition is ready in memory, the worker thread multiplies the partition with the input dense matrix. A thread processes one tile at a time and stores the intermediate result in a buffer al-

located in the local memory to reduce remote memory access.

To better utilize CPU cache, we process tiles of a partition in *super tiles* (Figure 2). The tile size of a sparse matrix is specified when the sparse matrix image is created and is relatively small to handle different numbers of columns in the dense matrices. A *super tile* is composed of tiles from multiple tile rows and its size is determined at runtime by three factors: the number of columns in the dense matrices, the CPU cache size and the number of threads that share the CPU cache. An optimal size for a *super tile* fills the CPU cache with the rows from the dense matrices involved in the computation with the *super tile*.

Load balancing also plays a key role in sparse matrix multiplication on many real-world graphs due to their power-law distribution in vertex degree. In FlashEigen, a worker thread first processes partitions originally assigned to the thread. When a worker thread finishes all of its own partitions, it steals partitions that have not been processed from other worker threads.

In spite of nearly random edge connection in a real-world graph, there exists regularity that allows vectorization to improve performance in sparse matrix dense matrix multiplication. For each non-zero entry, we need to multiply it with the corresponding row from the input dense matrix and add the result to the corresponding row in the output dense matrix. These operations can be accomplished by the vector CPU instructions such as AVX [?]. The current implementation relies on GCC’s auto-vectorization to translate the C code to the vector CPU instructions by predefining the matrix width in the code.

When accessing a sparse matrix on SSDs, we keep a set of memory buffers for I/O access to reduce the overhead of memory allocation. For a large sparse matrix, each tile row is fairly large, on the order of tens of megabytes. The operating system usually allocate a memory buffer for such an I/O size with *mmap()* and populates the buffer with physical pages when the buffer is used. It is computationally expensive to populate large memory buffers frequently. When accessing high-throughput I/O devices, such overhead can cause substantial performance loss. Therefore, we keep a set of memory buffers allocated previously and reuse them for new I/O requests. Because tile rows in a sparse matrix usually have different sizes, we resize a previously allocated memory buffer if it is too small for a new I/O request.

### 3.4 The vector subspace

The vector subspace required by an eigensolver is massive when the eigensolver computes eigenvalues of a billion-node graph or computes many eigenvalues of a

| name                   | operation   |
|------------------------|---|
| <i>MvTimesMatAddMv</i> | $CC \leftarrow \alpha \times AA \times B + \beta \times CC$ |
| <i>MvTransMv</i>       | $A \leftarrow \alpha \times t(AA) \times BB$                |
| <i>MvScale1</i>        | $BB \leftarrow \alpha \times AA$                            |
| <i>MvScale2</i>        | $BB \leftarrow AA \times \text{diag}(\text{vec})$           |
| <i>MvAddMv</i>         | $CC \leftarrow \alpha \times AA + \beta \times BB$          |
| <i>MvDot</i>           | $\text{vec}[i] \leftarrow t(AA[,i]) * BB[,i]$               |
| <i>MvNorm</i>          | $\text{vec} \leftarrow \text{norm\_col}(AA)$                |
| <i>CloneView</i>       | $AA[, \text{idxs}]$   |
| <i>SetBlock</i>        | $AA[, \text{idxs}] \leftarrow BB$                           |
| <i>MvRandom</i>        | $AA \leftarrow \text{rand\_init}$                           |
| <i>ConvLayout</i>      | $AA \leftarrow \text{conv\_layout}(BB)$                     |

Table 1: The dense matrix operations required by the Anasazi eigensolvers. *AA* and *BB* represents a tall dense matrix, *A* and *B* represents a small dense matrix,  $\alpha$  and  $\beta$  represents scalar variables.

multi-million-node graph. The number of vectors in the subspace increases with the number of required eigenvalues. Furthermore, a larger number of vectors in the subspace potentially improves the convergence rate of an eigensolver. The storage size required by the subspace is often larger than the sparse matrix for eigendecomposition on many real-world graphs. Therefore, FlashEigen stores these vectors on SSDs.

FlashEigen implements a set of dense matrix operations shown in Table 1. The Anasazi framework provides a set of programming interfaces that expose the vectors in the subspace to users as dense matrices and allow users to redefine the dense matrices and the operations on them. The first ten operations are the ones required by the Anasazi framework. The most computationally expensive operations are the two matrix multiplication operations: *MvTimesMatAddMv* and *MvTransMv*, mainly used for reorthogonalization to fix floating-point rounding errors. The eigensolvers use *CloneView* and *SetBlock* to access individual columns of a dense matrix, so we store the dense matrices in column major by default. However, the sparse matrix dense matrix multiplication described in Section 3.3 requires a row-major dense matrix to increase data locality. Thus, FlashEigen adds another operation *ConvLayout* to convert data layout in dense matrices, which converts a column-major matrix to a row-major matrix when it is passed to the SpMM operation.

External-memory dense matrix operations faces multiple challenges. Unlike sparse matrix multiplication, these dense matrix operations are less memory intensive. Even though SSDs are fast, their sequential I/O performance is still an order of magnitude slower than RAM. Furthermore, SSDs wears out after a certain amount of write. Even enterprise SSDs [18] only allows a small

number of DWPD (diskful writes per day). Therefore, FlashEigen optimizes dense matrix operations with three goals: (i) maximizing I/O throughput of SSDs, (ii) minimizing the amount of data read from SSDs, (iii) reducing SSD wearout.

### 3.4.1 The storage format of the vector subspace

FlashEigen stores multiple vectors in a dense matrix physically because Anasazi eigensolvers update multiple vectors of the subspace in an iteration thanks to the block extension. The number of vectors in a matrix is determined by the *block size* of a block eigensolver. As such, the subspace is composed of multiple tall-and-skinny (TAS) dense matrices.

FlashEigen stores each TAS matrix in a separate SAFS file to leverage the optimizations in SAFS. This guarantees that I/O accesses to the dense matrices are evenly distributed to all SSDs by SAFS, regardless of the number of SSDs and the subspace size. It also eases matrix creation and deletion by simply creating and deleting an SAFS file.

FlashEigen partitions a TAS matrix horizontally to assist in parallelization and external-memory access. Figure 4 (b) illustrates the format of an external-memory TAS matrix. Like a NUMA dense matrix in Figure 4 (a), an external-memory matrix is divided into multiple row intervals and data in a row interval is stored contiguously to generate large I/O requests, on the order of megabytes. The size of a row interval is chosen according to the number of columns in the matrix. Unlike a NUMA dense matrix, elements in a row interval of an external-memory matrix are stored in column-major order for easily accessing individual columns.

### 3.4.2 Parallelize matrix operations

All large dense matrices in FlashEigen are tall and skinny so we partition them horizontally for parallelization. All matrix operations in Table 1 allow a worker thread to process partitions of a matrix independently.

All of the matrix operations in Table 1 that outputs TAS matrices are embarrassingly parallelizable on the TAS matrices. In these operations, a row interval in the output matrix only depends on the same row interval from all of the TAS input matrices. Thus, the computation and data access to the TAS matrices are completely independent between row intervals. To parallelize these matrix operations, we assign one row interval at a time to a worker thread. When a worker thread gets a row interval, it owns the row interval and is responsible for accessing the data in the row interval from all of the TAS matrices and performing computation on them. When processing a row interval, a worker thread does not need

to access data from another row interval on SSDs.

Some of the operations do not output TAS matrices and their outputs depend on all row intervals of the input matrices. For example, *MvTransMv* outputs a small matrix. These operations can usually be split into two sub-operations: the first one performs computation on each row interval independently and outputs a small vector or a small matrix; the second one aggregates all of the small vectors or matrices and outputs a single small vector or matrix. The first sub-operation accounts for most of computation in such an operation and requires external-memory data access, so we parallelize it in the same fashion as the operations that output TAS matrices.

### 3.4.3 External memory access

I/O access for dense matrix operations is relatively simple. All matrix partitions have the same size and each operation requires to access all data in a TAS matrix, which results in sequential I/O access. For most of the matrix operations in Table 1, a worker thread reads data in a row interval asynchronously and perform computation when all data in the row interval is ready in memory. In this section, we describe some optimizations that aim at reducing memory consumption and achieving maximal I/O throughput from SSDs.

Keeping data in a row interval from all of the input TAS matrices potentially consumes a significant amount of memory if a matrix operation involves in many TAS matrices. Operations such as *MvTimesMatAddMv* and *MvTransMv* frequently take as input many vectors in the subspace, which is stored in multiple TAS dense matrices physically. The actual number of TAS matrices involved in the two operations varies between iterations and can grow to as large as several hundred when an eigensolver computes hundreds of eigenvalues. The storage size of a row interval is usually configured on the order of tens of megabytes to achieve I/O throughput from SSDs. When there are hundreds of dense matrices in the subspace, we may keep a substantial amount of data in memory. Reading only part of a partition results in many small reads and writes to SSDs because the matrices are organized in column-major order.

Instead, we break a large group of TAS matrices into multiple small groups to reduce memory consumption for these matrix operations. Figure 5 illustrates this optimization on *MvTimesMatAddMv* and *MvTransMv*. For *MvTimesMatAddMv*, we split the small dense matrix horizontally and each group of TAS matrices gets a partition of the small dense matrix. Each group generates an intermediate TAS matrix conceptually and we apply an addition operation on all of the intermediate matrices to generate the final result. As such, we perform computation on each group separately and only need to keep the

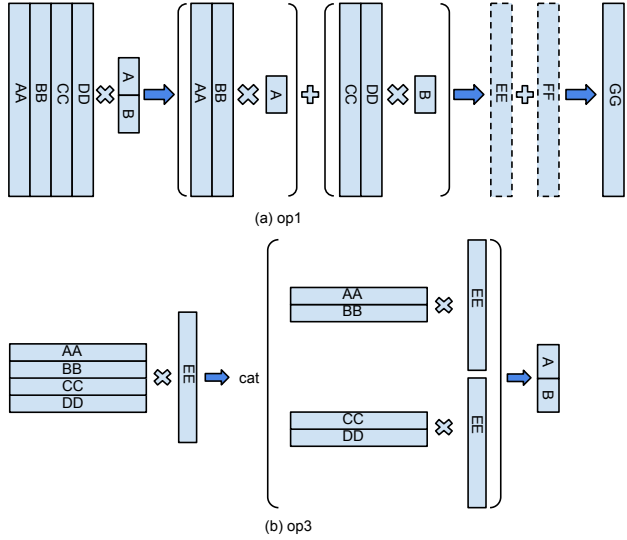


Figure 5: Break a large group of dense matrices in an operation into multiple small groups to reduce memory consumption. XX indicates a TAS matrix stored on SSDs and X indicates a small matrix stored in memory.

data in a row interval from all of the TAS matrices in a group. Therefore, memory consumption is determined by the group size instead of the number of TAS matrices involved in the operation. Materializing these intermediate matrices would result in large memory consumption if we store them in memory, or a large amount of I/O if we store them on SSDs. Instead, we only materialize part of the intermediate matrices and passes the materialized parts to the addition operation to generate the final result. We apply a similar strategy to *MvTransMv*, which requires each group to share the same TAS matrix in the right operand. Each group generates a small matrix that is small enough to be kept in memory. To minimize I/O, we share I/O for accessing the TAS matrix in the right operand.

Like sparse matrix multiplication, we maintain a per-thread memory buffer pool for I/O access to reduce the overhead of memory allocation when accessing dense matrices on SSDs. To increase I/O throughput, we access data in dense matrices on SSDs with large I/O requests. Allocating a large memory buffer for each I/O request causes the operating system to populate memory with physical pages when the buffer is used and this is a computationally expensive operation. Therefore, we maintain a pool of memory buffers with physical pages populated in advance and associate each I/O request with a buffer from the set. We maintain such a pool for each worker thread to minimize locking overhead.

### 3.4.4 Matrix caching

FlashEigen deploys two forms of matrix caching to reduce I/O to SSDs. In the first case, FlashEigen worker threads cache part of a TAS matrix locally. In the other case, FlashEigen can also cache the most recent TAS matrix in the vector subspace.

Caching part of a TAS matrix read from SSDs benefits some of the matrix operations. One example is the optimization for *op3* in section 3.4.3, which breaks a large group of dense matrices into multiple subgroups and the matrix in the right operand is shared by all of the subgroups. A worker thread only needs to cache data in a row interval of the right matrix that is currently being processed because a thread processes one row interval at a time and each row interval of the TAS matrices is processed only once. Therefore, a worker thread can buffers the data in a row interval of a matrix locally and accessing the buffered data doesn't incur any locking overhead.

When we buffer the recent portions, we need to give each matrix a data identifier to identify its data, so we can recognize which portion of data can be reused. For certain operations, even though a new matrix is created, the data inside remains the same. A typical example is transpose. The identifier we give to each matrix should identify the data inside a matrix instead of individual matrices, so a transposed matrix and its original matrix should share the same identifier.

FlashEigen also caches the most recent TAS matrix in the vector subspace if the RAM of a machine is sufficient to accommodate the entire matrix. When a new matrix in the vector subspace is generated by sparse matrix multiplication, an eigensolver needs to perform a sequence of operations on it, which includes reorganization. By caching the matrix in memory, we can significantly reduce the amount of data written to SSDs.

## 4 Experimental Evaluation

We evaluate the performance of the SSD-based FlashEigen on multiple real-world billion-scale graphs including a web-page graph with 3.4 billion vertices. We first evaluate the performance of the two most computationally intensive computation in the eigensolvers: sparse matrix dense matrix multiplication and dense matrix multiplication. We demonstrate the effectiveness of the optimizations on the two operations and compare the performance of our external-memory implementation with multiple in-memory implementations: (i) our in-memory implementations, (ii) MKL and (iii) Trilinos. We then evaluate the overall performance of FlashEigen and compare with the original Anasazi eigensolvers. We further demonstrate the scalability of FlashEigen on a web graph of 3.4 billion vertices and 129 billion edges.



| Graph datasets        | # Vertices | # Edges | Directed |
|-----------------------|------------|---------|----------|
| Twitter [13]          | 42M        | 1.5B    | Yes      |
| Friendster [27]       | 65M        | 1.7B    | No       |
| KNN distance graph [] | 62M        | 12B     | No       |
| Page [25]             | 3.4B       | 129B    | Yes      |

Table 2: Graph data sets.

We conduct all experiments on a non-uniform memory architecture machine with four Intel Xeon E7-4860 processors, clocked at 2.6 GHz, and 1TB memory of DDR3-1600. Each processor has 12 cores. The machine has three LSI SAS 9300-8e host bus adapters (HBA) connected to a SuperMicro storage chassis, in which 24 OCZ Intrepid 3000 SSDs are installed. The 24 SSDs together are capable of delivering 12 GB/s for read and 10 GB/s for write at maximum. The machine runs Linux kernel v3.13.0. We use 48 threads for most of experiments by default.

We use the real-world graphs in Table 2 for evaluation. The largest graph is the page graph with 3.4 billion vertices and 129 billion edges. The smallest graph we use has 42 million vertices and 1.5 billion edges. Twitter and Friendster are social network graphs. The KNN distance graph is a symmetrized 100-nearest neighbor adjacency graph with cosine distance as the edge weight. The distance graph is generated over all frames of the Babel Tagalog corpus, commonly used in speech recognition. Majority of the vertices in this graph has degree between 100 to 1000, so this graph does not follow the power-law distribution in vertex degree. The page graph is clustered by domain, generating good CPU cache hit rates in sparse matrix dense matrix multiplication.

For performance evaluation, we implement an in-memory implementation of both sparse matrix multiplication and dense matrix multiplication. Therefore, our FlashEigen eigensolver is able to run both in memory and on SSDs. In the following sections, we denote the eigensolver in memory by FE-IM and the eigensolver on SSDs with FM-SEM.

## 4.1 Sparse matrix multiplication

This section evaluates the performance of the semi-external-memory (SEM) implementation of SpMM in FlashEigen. We first evaluate the effectiveness of the optimizations on the SpMM. Then we compare its performance with that of the Intel MKL and Trilinos implementations.

### 4.1.1 Optimizations on SpMM

We first deploy a set of memory optimizations to implement a fast in-memory sparse matrix multiplication and then deploy a set of I/O optimizations to further speed

up this operation in semi-external memory. We apply the memory and I/O optimizations incrementally to illustrate their effectiveness.

For memory optimizations, we start with an implementation that performs sparse matrix multiplication on a sparse matrix in the CSR format and apply the optimizations incrementally in the following order:

- partition dense matrices for NUMA (*NUMA*),
- partition the sparse matrix in both dimensions into tiles of  $16K \times 16K$  (*Cache blocking*),
- organize multiple physical tiles into a super tile to fill CPU cache (*Super tile*),
- use CPU vectorization instructions (*Vec*),
- allocate a local buffer to store the intermediate result of multiplication of tiles and the input dense matrix (*Local write*),
- combine the SCSR and COO format to reduce the number of conditional jump CPU instructions (*SCSR+COO*),

Figure 6 shows that almost all of these optimizations have positive effect on sparse matrix multiplication and all optimizations together speed up the operation by 2 – 4 times. The degree of effectiveness varies significantly between different graphs and different numbers of columns in the dense matrices. For example, the NUMA optimization is more effective when the dense matrices have more columns because more columns in the dense matrices require more memory bandwidth. Cache blocking is very effective when the dense matrices have fewer columns because it can effectively increase CPU cache hits. When there are more columns in the dense matrices, data locality improves and cache blocking becomes less effective. When there are too many columns, the rows from the input and output matrices can no longer be in the CPU cache. Thus, it even has a little negative effect on the Friendster graph when the dense matrices have 16 columns. However, we never use dense matrices with more than four columns in sparse matrix multiplication in the KrylovSchur eigensolver. With all optimizations, we have a fast in-memory sparse matrix dense matrix multiplication, denoted by FE-IM SpMM.

### 4.1.2 SpMM performance

We then evaluate the performance of the SEM SpMM in FlashEigen and compare its performance with FE-IM SpMM, the MKL implementation and the Trilinos implementation (Figure 7). We only show the performance of SpMM on the Friendster graph and the performance on the other graphs is similar. The MKL and Trilinos SpMM cannot run on the page graph.

Our SEM SpMM has performance comparable to FE-IM SpMM, while both FE-IM SpMM and FE-SEM

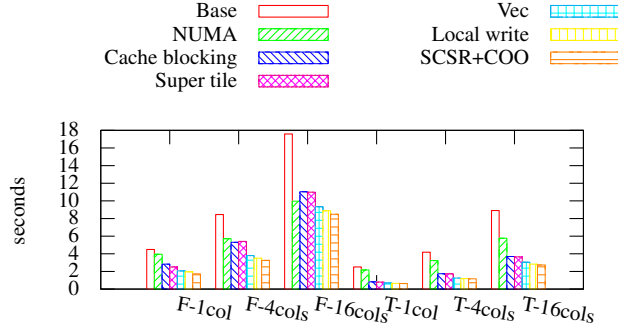


Figure 6: The effectiveness of the SpMM optimizations on the Friendster graph (F) and the Twitter graph (T) for different numbers of columns in the dense matrices.

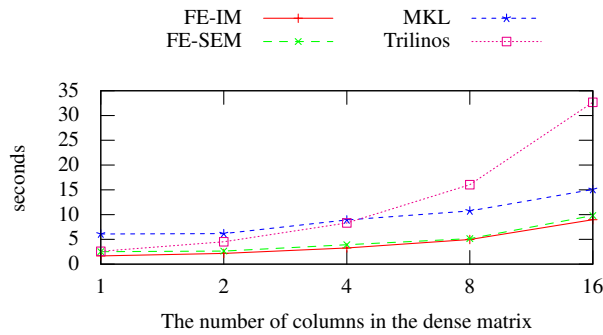


Figure 7: The runtime of in-memory SpMM (FE-IM) and SEM-SpMM (FE-SEM) in the FlashEigen, the MKL and the Trilinos implementation on the Friendster graph.

SpMM outperforms the MKL and Trilinos implementations. On the Friendster graph, FE-SEM SpMM achieves 60% performance of FE-IM SpMM when the dense matrix has only one column and the performance gap narrows as the number of columns in the dense matrices increases. The Trilinos SpMM is optimized for sparse matrix vector multiplication (SpMV). But even for SpMV, our IM-SpMM outperforms Trilinos by 36%. The MKL SpMM performs better when the dense matrices have more columns, but our implementations can still outperform MKL by 2 – 3 times in most settings.

## 4.2 Dense matrix multiplication

This section evaluates the performance of dense matrix multiplication, the other computationally intensive operation in an eigensolver. For dense matrix multiplication, we focus on I/O optimizations, so we evaluate the effectiveness of the I/O optimizations on this operation. Then we compare the performance of our in-memory and external-memory implementations with the ones in Intel MKL and Trilinos.

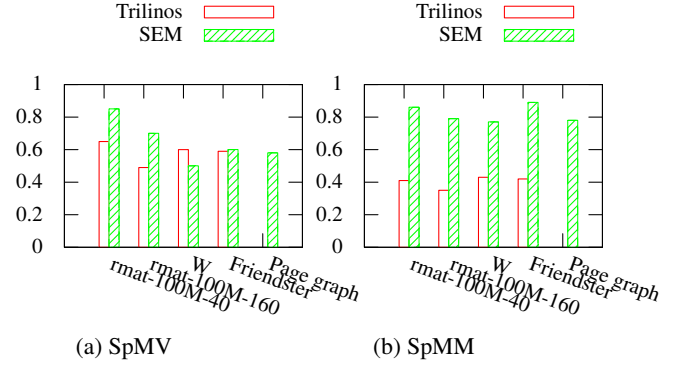


Figure 8: The performance of Trilinos and FlashEigen-SEM sparse matrix multiplication relative to FlashEigen-IM sparse matrix multiplication. In sparse matrix dense multiplication (SpMM), there are four columns in the dense matrix.

In eigendecomposition, there are two forms of dense matrix multiplication. The first form, shown by *op1* in Table 1, multiplies a tall-and-skinny dense matrix of  $n \times m$  with a small dense matrix of  $m \times b$  and outputs a tall-and-skinny dense matrix of  $n \times b$ , where  $n$  is the size of the eigenvalue problem,  $m$  is the number of existing vectors in the subspace and  $b$  is the block size of the eigensolver. The second form, shown by *op3*, multiplies a transpose of a tall-and-skinny dense matrix of  $n \times m$  with another tall-and-skinny dense matrix of  $n \times b$  and outputs a small matrix. In both forms,  $m$  varies from one block size to the maximal subspace size specified by a user and is increased by one block size in each iteration. In the experiments, we set  $n$  to 60M, roughly the size of eigenvalue problems in Table 2,  $b$  to 4 and vary  $m$  from 4 to 512. This setting of  $b$  and  $m$  is used in the experiments of our external-memory KrylovSchur eigensolver in the next section.

### 4.2.1 Optimizations on dense matrix multiplication

We illustrate the most effective I/O optimizations on dense matrix multiplication. We start with a basic implementation of matrix multiplication in SAFS and deploy the optimizations on SAFS and matrix multiplication incrementally in the following order:

- use different random striping orders for each file (*diff strip*),
- use a per-thread buffer pool to allocate memory for I/O (*buf pool*),
- use one I/O thread per NUMA node (*IIOT*),
- use I/O polling in worker threads (*polling*),
- use 8MB for the maximal block size in the kernel (*max block*),

The effectiveness of the optimizations on external memory dense matrix multiplication is shown in Figure

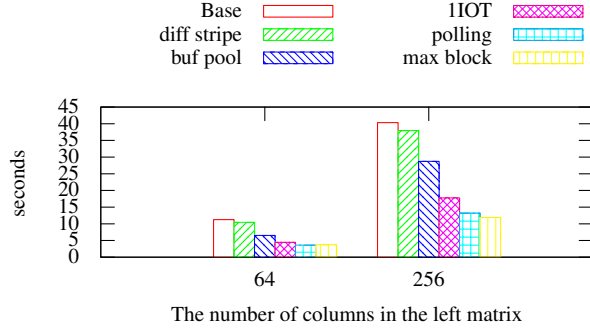


Figure 9: The effectiveness of I/O optimizations on dense matrix multiplication.

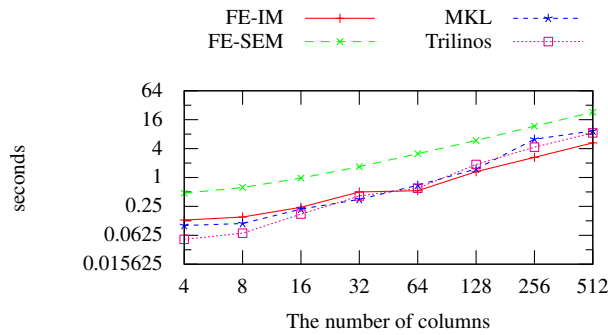


Figure 10: The runtime of dense matrix multiplication in *op1*. We compare in-memory (FE-IM) and external-memory (FE-EM) implementations in FlashEigen with the MKL and Trilinos implementations.

9. We only demonstrate their effectiveness on the second form of dense matrix multiplication and their effectiveness in the first form is very similar. As shown in Figure 9, using a per-thread buffer pool and a smaller number of I/O threads has the most significant performance improvement. By combining all of the optimizations together, we increase the performance by a factor of up to four. This also indicates the importance of reducing the overhead of thread context switches in high-throughput I/O access.

#### 4.2.2 Dense matrix multiplication performance

Figure 10 show the performance of the in-memory and external-memory dense matrix multiplication in the first form. We omit the performance result of dense matrix multiplication in the second form because it is very similar to the first form and MKL cannot parallelize it. The external-memory multiplication in FlashEigen is roughly 3-6 times slower than its in-memory counterpart. In the dense matrix multiplication of the first form, the in-memory implementation outperforms MKL and Trilinos

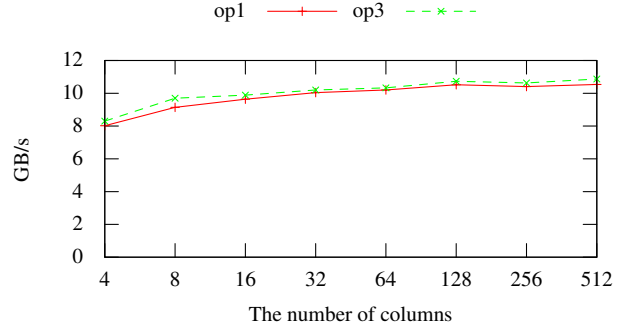


Figure 11: The average I/O throughput in dense matrix multiplication on the SSD array.

when the number of the columns get larger and MKL does not have a parallel implementation for the dense matrix multiplication of the second form.

The external-memory dense matrix multiplication has almost saturated the I/O bandwidth of the SSDs (Figure 11). The average I/O throughput reaches 10.87GB/s from the entire SSD array or 464MB/s per SSD, while the peak throughput of an SSD is approaching 500MB/s, which is close to the maximal I/O throughput of 540MB/s per SSD, advertised by the SSD vendor. This also indicates that the SSDs are the bottleneck for the dense matrix multiplication in the eigensolver. This is not surprising because the sequential I/O performance of SSDs is an order of magnitude smaller than RAM.

### 4.3 The KrylovSchur eigensolver in FlashEigen

In this section, we focus on evaluating the performance of the KrylovSchur eigensolvers in FlashEigen. KrylovSchur is not only the fastest in-memory eigensolver on the graphs in Table 2 among all Anasazi eigensolvers, but also generates the least I/O, especially writes, to SSDs. Reducing I/O is essential to achieve performance and reduce SSD wearout. We evaluate our external-memory eigensolver and compare it with its in-memory counterpart as well as the original KrylovSchur eigensolver in the Anasazi framework.

The KrylovSchur eigensolver has two important parameters: the subspace size and the block size. They significantly affect the convergence of the KrylovSchur eigensolver. A reasonably large subspace size and block size accelerates its convergence. However, a larger subspace increases memory consumption of the eigensolver as well as computation and I/O complexity in a single matrix operation. A larger block size increases memory consumption of FlashEigen.

For the experiments below, we select the values for

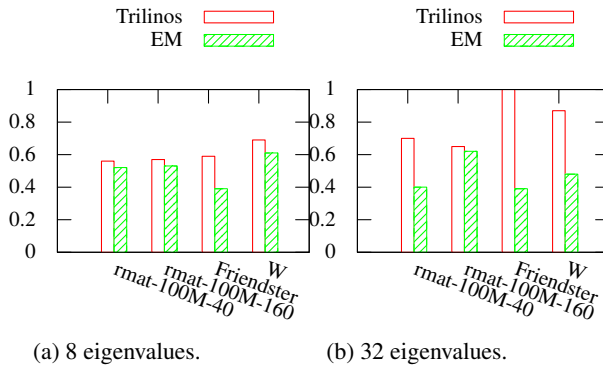


Figure 12: The performance of the Trilinos KrylovSchur and FlashEigen-EM KrylovSchur relative to the FlashEigen-IM KrylovSchur.

the two parameters that achieve the best runtime performance for the eigensolvers. We assume that our setting is not constrained by memory size available to the machine. Because sparse matrix in Trilinos is not optimized for the dense matrix with more than one column, we use 1 as the block size and  $2 \times ev$  as the number of blocks for most of the graphs in the original KrylovSchur eigensolver, where  $ev$  is the number of the eigenvalues to compute. For the FlashEigen KrylovSchur eigensolver, we choose the subspace size and the block size to reduce the amount of I/O to SSDs. we use 1 as the block size and  $2 \times ev$  as the number of blocks when computing a small number of eigenvalues and use 4 as the block size and  $ev$  as the number of blocks. Therefore, the FlashEigen eigensolver uses the subspace twice as large as the one used by the original KrylovSchur eigensolver when computing a large number of eigenvalues. However, the eigenvalues of the graph  $W$  are very close to each other, so we have to use a much larger subspace to have the eigensolver to converge or converge faster. For the  $W$  graph, we use the subspace four times larger than the ones used for other graphs. Therefore, we can trade off the runtime performance with memory consumption in eigendecomposition.

#### 4.3.1 Performance of eigensolvers

We evaluate the performance of our SEM eigensolver and compare its performance with our in-memory eigensolver and the original KrylovSchur eigensolver. We compute different numbers of eigenvalues on the three smaller graphs in Table 2. Only our SEM eigensolver is able to compute eigenvalues on the page graph on the 1TB-memory machine.

Our SEM eigensolver achieves at least 40% performance of our in-memory eigensolver, while the in-memory eigensolver outperforms the original KrylovSchur eigensolver (Figure 12). The SEM eigensolver is more efficient to compute a small number

| #eigenvalues | runtime   | memory | read  | write |
|--------------|-----------|--------|-------|-------|
| 8            | 4.2 hours | 120GB  | 145TB | 4TB   |

Table 3: The performance and resource consumption of computing eigenvalues on the page graph.

of eigenvalues and is able to achieve around 50% performance of our in-memory eigensolver. SpMM and reorthogonalization account for most of computation time when computing a small number of eigenvalues, but reorthogonalization eventually dominates the eigendecomposition for computing many eigenvalues. Because external-memory dense matrix multiplication is several times slower than the in-memory implementations, reorthogonalization accounts for over 90% of runtime in the SEM eigensolver for computing a large number of eigenvalues. For many spectral analysis tasks, users only require a small number of eigenvalues.

The SEM eigensolver uses a small fraction of memory used by its in-memory counterparts and the original Trilinos eigensolver and its memory consumption remains roughly the same as the number of eigenvalues computed by the eigensolvers increases. A small memory consumption provides two benefits. First, FlashEigen is able to scale to a much larger eigenvalue problem. The second benefit is that FlashEigen gives users more freedom to choose the subspace size that gives the fastest convergence in a given eigenvalue problem because SSDs significantly increases memory available to the eigensolver. We have to point out that our experiments assume that we choose the subspace size that is not constrained by the memory size in a machine.

#### 4.3.2 Scale to billion-node graphs

We evaluate the scalability of FlashEigen with the page graph with 3.4 billion vertices and 129 billion edges. Because the page graph is a directed graph, its adjacency matrix is asymmetric and we perform singular value decomposition (SVD) on the adjacency matrix instead of simple eigendecomposition. For the page graph, we use 2 for the block size and  $2 \times ev$  for the number of blocks because sparse matrix multiplication is completely bottlenecked by SSDs. Neither the in-memory eigensolver nor the original Trilinos eigensolver is able to compute eigenvalues on the page graph with 1TB RAM.

FlashEigen computes a fairly large number of eigenvalues within a reasonable amount of time and consumes a fairly small amount of resources given the large size of the eigenvalue problem. The average I/O throughput during the computation of 8 eigenvalues is about 10GB/s, which is very close to the maximal I/O throughput provided by the SSD array. Given the relative small mem-

ory footprint, we are able to scale FlashEigen to a much larger eigenvalue problem on our 1TB-RAM machine.

## 5 Conclusions

We present an external-memory framework called FlashEigen using a large array of commodity SSDs to solve eigenvalue problems at the billion scale. FlashEigen utilizes the Anasazi framework to get state-of-art eigensolver implementations so that we can focus on optimizations on sparse matrix multiplication and dense matrix multiplication on SSDs.

We implement a sparse matrix dense matrix multiplication in the semi-external memory fashion. That is, we keep the sparse matrix on SSDs and the dense matrices in memory. We deploy a set of memory and I/O optimizations so that the sparse matrix dense matrix multiplication has performance comparable to its in-memory counterparts while significantly outperforming the MKL and Trilinos implementation. The semi-external sparse matrix multiplication is able to saturate either CPU or SSDs or both, which suggests that we have achieved the maximal performance from the existing hardware.

We further implement and optimize external-memory matrix multiplication for FlashEigen. When computing eigenvalues on many real-world graphs, the storage size required by the subspace in an eigensolver is massive. Therefore, we keep the subspace on the SSD array and deploy a set of I/O optimizations on dense matrix multiplication. With the I/O optimizations, we saturate the SSDs in dense matrix multiplication and achieve the maximal performance from the existing hardware. However, the SSD array is an order of magnitude slower than RAM, so external-memory dense matrix multiplication is about three or four times slower than the state-of-art in-memory dense matrix multiplication.

We implement our external-memory eigensolver with the semi-external memory sparse matrix multiplication and the external-memory dense matrix multiplication. Our experiments show that our external-memory eigensolver achieves at least 30% of the performance of its in-memory counterparts. For a small number of eigenvalues, which is the most common case for spectral analysis, our external-memory eigensolver has less than 50% performance loss. We further show that our external-memory eigensolver is able to scale a graph with 3.4 billion vertices and 129 billion edges. It finishes eigendecomposition within a reasonable amount of time and consumes a fairly small amount of resources. This suggests that our external-memory eigensolver is able to scale to even a larger eigenvalue problem in our 1TB-RAM machine.

We are able to scale to much larger graphs. Given the same amount of resources, SSDs significantly extends the memory capacity and give users the freedom

of choosing the optimal subspace size for better convergence. Our solution also works better for relatively denser graphs. Our solution works better for computing a small number of eigenvalues.

## 6 Acknowledgments

This work is partially supported by NSF ACI-1261715, DARPA GRAPHS N66001-14-1-4028 and DARPA SIMPLEX program through SPAWAR contract N66001-15-C-4041.

## References

- [1] ABELLO, J., BUCHSBAUM, A. L., AND WESTBROOK, J. R. A functional approach to external graph algorithms. In *Algorithmica* (1998), Springer-Verlag.
- [2] AKTULGA, H. M., BULUÇ, A., WILLIAMS, S., AND YANG, C. Optimizing sparse matrix-multiple vectors multiplication for nuclear configuration interaction calculations. In *Proceedings of the 2014 IEEE 28th International Parallel and Distributed Processing Symposium* (2014).
- [3] ANDERSON, E., BAI, Z., BISCHOF, C., BLACKFORD, S., DEMMEL, J., DONGARRA, J., DU CROZ, J., GREENBAUM, A., HAMMARLING, S., MCKENNEY, A., AND SORENSEN, D. *LAPACK Users' Guide*, third ed. Society for Industrial and Applied Mathematics, Philadelphia, PA, 1999.
- [4] ARBENZ, P., HETMANIUK, U. L., LEHOUCQ, R. B., AND TUMINARO, R. S. A comparison of eigensolvers for large-scale 3D modal analysis using AMG-preconditioned iterative methods. *International Journal for Numerical Methods in Engineering* (2005).
- [5] ARBENZ, P., HETMANIUK, U. L., LEHOUCQ, R. B., AND TUMINARO, R. S. A comparison of eigensolvers for large-scale 3D modal analysis using AMG-preconditioned iterative methods. *International Journal for Numerical Methods in Engineering* (2005).
- [6] BOMAN, E. G., DEVINE, K. D., AND RAJAMANICKAM, S. Scalable matrix computations on large scale-free graphs using 2D graph partitioning. In *Proceedings of the International Conference on High Performance Computing, Networking, Storage and Analysis* (2013).
- [7] CALVETTI, D., REICHEL, L., AND SORENSEN, D. C. An implicitly restarted lanczos method for large symmetric. . . *ETNA* 2 (1994), 1–21.
- [8] DEAN, J., AND GHEMAWAT, S. MapReduce: Simplified data processing on large clusters. In *Proceedings of the 6th Conference on Symposium on Operating Systems Design & Implementation - Volume 6* (2004).
- [9] HERNANDEZ, V., ROMAN, J. E., AND VIDAL, V. SLEPc: A scalable and flexible toolkit for the solution of eigenvalue problems. *ACM Trans. Math. Softw.* (2005).
- [10] HEROUX, M. A., BARTLETT, R. A., HOWLE, V. E., HOEKSTRA, R. J., HU, J. J., KOLDA, T. G., LEHOUCQ, R. B., LONG, K. R., PAWLOWSKI, R. P., PHIPPS, E. T., SALINGER, A. G., THORNQUIST, H. K., TUMINARO, R. S., WILLENBRING, J. M., WILLIAMS, A., AND STANLEY, K. S. An overview of the Trilinos project. *ACM Trans. Math. Softw.* (2005).
- [11] IM, E.-J., YELICK, K., AND VUDUC, R. Sparsity: Optimization framework for sparse matrix kernels. *Int. J. High Perform. Comput. Appl.* (2004).

- [12] KANG, U., MEEDER, B., AND FALOUTSOS, C. Spectral analysis for billion-scale graphs: Discoveries and implementation. In *Proceedings of the 15th Pacific-Asia Conference on Advances in Knowledge Discovery and Data Mining - Volume Part II* (2011).
- [13] KWAK, H., LEE, C., PARK, H., AND MOON, S. What is twitter, a social network or a news media? In *Proceedings of the 19th International Conference on World Wide Web* (2010).
- [14] LANCZOS, C. An iteration method for the solution of the eigenvalue problem of linear differential and integral operators. *Journal of Research of the National Bureau of Standards* (1950).
- [15] LEHOUCQ, R., SORENSEN, D., AND YANG, C. *ARPACK Users' Guide*. Society for Industrial and Applied Mathematics, 1998.
- [16] LESKOVEC, J., LANG, K. J., DASGUPTA, A., AND MAHONEY, M. W. Community structure in large networks: Natural cluster sizes and the absence of large well-defined clusters. *Internet Mathematics* 6, 1 (2009), 29–123.
- [17] NG, A. Y., JORDAN, M. I., AND WEISS, Y. On spectral clustering: Analysis and an algorithm. In *Advances in Neural Information Processing Systems 14*. 2002.
- [18] OCZ Intrepid 3000. <http://ocz.com/enterprise/intrepid-3000-sata-ssd>, Accessed 11/5/2015.
- [19] PAN, V. Y., AND CHEN, Z. Q. The complexity of the matrix eigenproblem. In *Proceedings of the Thirty-first Annual ACM Symposium on Theory of Computing* (1999).
- [20] SORENSEN, D. C. Implicitly restarted ARNOLDI/LANCZOS methods for large scale eigenvalue calculations. Tech. rep., 1996.
- [21] STEWART, G. W. A KrylovSchur algorithm for large eigenproblems. *SIAM Journal on Matrix Analysis and Applications* (2002).
- [22] SUSSMAN, D. L., TANG, M., FISHKIND, D. E., AND PRIEBE, C. E. A consistent adjacency spectral embedding for stochastic blockmodel graphs. *Journal of the American Statistical Association* (2012).
- [23] TANG, L., HUANG, Q., LLOYD, W., KUMAR, S., AND LI, K. RIPQ: Advanced photo caching on flash for Facebook. In *13th USENIX Conference on File and Storage Technologies (FAST 15)* (Feb. 2015).
- [24] TSOURAKAKIS, C. Fast counting of triangles in large real networks without counting: Algorithms and laws. In *Data Mining, 2008. ICDM '08. Eighth IEEE International Conference on* (2008).
- [25] Web graph. <http://webdatacommons.org/hyperlinkgraph/>, Accessed 4/18/2014.
- [26] WILLIAMS, S., OLIKER, L., VUDUC, R., SHALF, J., YELICK, K., AND DEMMEL, J. Optimization of sparse matrix-vector multiplication on emerging multicore platforms. In *Proceedings of the 2007 ACM/IEEE Conference on Supercomputing* (2007).
- [27] YANG, J., AND LESKOVEC, J. Defining and evaluating network communities based on ground-truth. In *Proceedings of the ACM SIGKDD Workshop on Mining Data Semantics* (2012).
- [28] YOO, A., BAKER, A. H., PEARCE, R., AND HENSON, V. E. A scalable eigensolver for large scale-free graphs using 2D graph partitioning. In *Proceedings of 2011 International Conference for High Performance Computing, Networking, Storage and Analysis* (2011).
- [29] ZHENG, D., BURNS, R., AND SZALAY, A. S. Toward millions of file system IOPS on low-cost, commodity hardware. In *Proceedings of the International Conference on High Performance Computing, Networking, Storage and Analysis* (2013).
- [30] ZHENG, D., MHEMBERE, D., BURNS, R., VOGELSTEIN, J., PRIEBE, C. E., AND SZALAY, A. S. FlashGraph: Processing billion-node graphs on an array of commodity SSDs. In *13th USENIX Conference on File and Storage Technologies (FAST 15)* (2015).
- [31] ZHOU, Z., SAULE, E., AKTULGA, H., YANG, C., NG, E., MARIS, P., VARY, J., AND CATALYUREK, U. An out-of-core eigensolver on SSD-equipped clusters. In *Cluster Computing (CLUSTER), 2012 IEEE International Conference on* (2012).